

Spin-polarized Majorana Bound States inside a Vortex Core in Topological Superconductors

Yuki NAGAI, Hiroki NAKAMURA, and Masahiko MACHIDA

CCSE, Japan Atomic Energy Agency, 5-1-5 Kashiwanoha, Kashiwa, Chiba 277-8587, Japan

We reveal that Majorana bound states inside the vortex core in an odd-parity topological superconductivity classified as “pseudo-scalar” type in the gap function are distinctly spin-polarized by solving the massive Dirac Bogoliubov-de Gennes (BdG) equation considering the spin-orbit coupling. This result is universal for “Dirac superconductivity” whose rotational degree of freedom is characterized by the total angular momentum $\mathbf{J} = \mathbf{S} + \mathbf{L}$ and in marked contrast to the spin-degeneracy of the core bound states as the consequence of the conventional BdG equation. The spin-polarized vortex core can be easily detected by spin-sensitive probes such as the neutron scattering and other measurements well above the first critical magnetic field H_{c1} .

1. Introduction

The discovery of topological superconductors opened a new research avenue on superconducting states. The topologically-protected nature together with $U(1)$ broken symmetry results in gapless zero-energy quasi-particles identified as Majorana fermions at surface edges, while the superconducting gap opens in the bulk body. The emerged Majorana fermion is a counterintuitive particle whose annihilation and creation operators are identical. Such a unique particle has a promising role in topological quantum computing utilizing its non-Abelian statistics.¹⁾ This fascinating feature has highly stimulated many theorists and experimentalists to intensively study the topological superconductivity.^{2–12)} However, its research history is not so long as the topological insulator, and most of rich physics still remain elusive.

Very recently, experimental works on topological insulators, Bi_2Se_3 and SnTe have revealed that they turn into superconductors with carrier doping. Their superconducting gap functions are not conventional since zero-bias conductance peaks (ZBCP’s) have been detected by the point contact spectroscopy.^{13,14)} The ZBCP is known to be observed in not only unconventional non- s -wave superconductors but also topological superconductors.^{13–20)} The latter typical example is the chiral p -wave topological superconductor such as Sr_2RuO_4 , in which gapless quasi-particles assigned as Majorana fermions induce ZBCP’s.^{21–23)} Accordingly, ZBCP’s observed in $\text{Cu}_x\text{Bi}_2\text{Se}_3$ ($T_c \sim 3\text{K}$) and $\text{Sn}_{1-x}\text{In}_x\text{Te}$ ($T_c \sim 1.2\text{K}$) can be also regarded to be originated from their non-trivial topology.

In topological superconductors, the Majorana fermion appears at not only surface edges but also vortex cores. Its emergence inside the vortex core has been numerically confirmed by using the Bogoliubov-de Gennes (BdG) formalism for p -wave triplet superconductors.^{24,25)} Since the vortex is a movable object, the Majorana fermion confined inside the core is also mobile. The character is hopeful for the topological

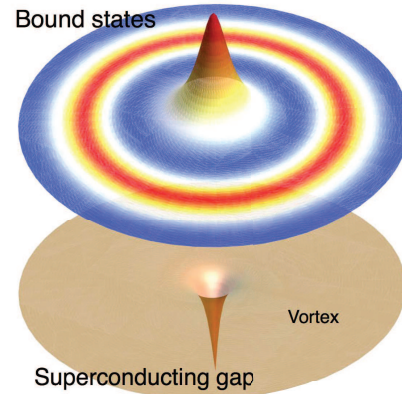


Fig. 1. (Color online) Spin-polarized Majorana bound states. The red (blue) region denotes dominance of up-spin (down-spin) component.

quantum computing, because vortex manipulation techniques have been rapidly developed in the last decade. In this paper, we present a new insight on the Majorana bound fermion inside the vortex core. We reveal that the Majorana state is spin-polarized in topological superconductors originated from strong spin-orbit coupling. Such a case is not particular but rather universal, since the spin degeneracy supposed to be kept in the conventional BdG formalism is generally broken when spin and orbital angular momenta are coupled.

Two orbital degrees of freedom in addition to two spin ones are required in a minimum model of the topological superconductivity under the strong spin-orbit coupling.^{5,14,26)} Then, the starting BdG Hamiltonian corresponds to a massive Dirac-type one including off-diagonal gap functions, in which the Lorentz transformation invariance together with anti-

commutation between two fermions gives mathematical restrictions on possible gap functions. As described in Ref. 27, the allowed gap functions are characterized as a scalar, a pseudo-scalar, and polar-vectors, when considering the on-site Cooper pairing. The polar-vector case always produces a specific direction around which the rotational isotropy is broken below the superconducting transition. Consequently, the restrictions allow six kinds of pairings, which are classified into two even-parity pairings being not topological and four odd parity ones being topological. In $\text{Cu}_x\text{Bi}_2\text{Se}_3$, Sasaki *et al.* theoretically examined which type among these pairings successfully reproduces observed ZBCP's and suggested that the odd-parity spin-triplet pairing is the most likely. Another superconductor, $\text{Sn}_{1-x}\text{In}_x\text{Te}$ can be also checked by the same scheme.¹³⁾ In this paper, we study vortex core bound-states in an odd-parity superconductor whose gap function is characterized as a ‘‘pseudo-scalar’’ keeping the rotational isotropy in all directions. In this case, the zero-energy Majorana bound states emerge inside the vortex cores as well as surface edges, and the core-bound Majorana fermion is distinctly spin-polarized around the vortex line. In other topological cases such as polar vectors, the spin-polarization becomes obscure since the rotational isotropy is broken around the vortex line and the polarized core states are mixed with each other. The Majorana fermions are also spin-polarized in topological wires.²⁸⁾ Consequently, we address that the spin-polarized character of the Majorana bound states is universal. We analytically and numerically demonstrate the spin-polarized vortex core and discuss the theoretical mechanism as well as its experimental detection possibilities.

2. Model

An effective theory for the topological superconductor with the intrinsic spin-orbit coupling is given by the massive Dirac type of BdG Hamiltonian together with a Nambu representation for the two orbital degrees of freedom as

$$H = \int d\mathbf{r} \begin{pmatrix} \bar{\psi}(\mathbf{r}) & \bar{\psi}_c(\mathbf{r}) \end{pmatrix} \begin{pmatrix} \hat{H}^-(\mathbf{r}) & \Delta^-(\mathbf{r}) \\ \Delta^+(\mathbf{r}) & \hat{H}^+(\mathbf{r}) \end{pmatrix} \begin{pmatrix} \psi(\mathbf{r}) \\ \psi_c(\mathbf{r}) \end{pmatrix}, \quad (1)$$

where

$$\hat{H}^\pm(\mathbf{r}) = M(-i\nabla) + \sum_{\nu=1}^3 P_\nu(-i\nabla)\gamma^\nu \pm P_0(-i\nabla)\gamma^0. \quad (2)$$

Here, γ^j is a 4×4 Dirac gamma matrix which can be described as $\gamma^0 = \hat{\sigma}_z \otimes 1$, $\gamma^{i=1,2,3} = i\hat{\sigma}_y \otimes \hat{s}_i$, and $\gamma^5 = \hat{\sigma}_x \otimes 1$ with 2×2 Pauli matrices $\hat{\sigma}_i$ in the orbital space and \hat{s}_i in the spin space, $\psi(\mathbf{r})$ is the Dirac spinor, $\bar{\psi}(\mathbf{r}) \equiv \psi^\dagger(\mathbf{r})\gamma^0$, $\bar{\psi}_c(\mathbf{r}) \equiv \psi_c^\dagger(\mathbf{r})\gamma^0$, and $\psi_c \equiv C\bar{\psi}^T$, where $C(\equiv i\gamma^2\gamma^0)$ is the representative matrix of the charge conjugation. M and P_ν are functions whose forms depend on the materials. Δ^- is a gap function, and $\Delta^+ \equiv \gamma^0(\Delta^-)^\dagger\gamma^0$. Considering only the on-site pairing interaction, the possible gap form is reduced to six types of functions as seen in Table I of Ref. 27. These gap functions are classified into a pseudo-scalar, a scalar, and a polar vector (four-vector)

associated with the Lorentz transformation,

$$\Delta^- = \Delta_0, \Delta_0\gamma^5, \Delta_0\hat{x}\gamma^5, \quad (3)$$

where Δ_0 is a scalar, the Feynman slash \hat{x} is defined by $\sum_\mu \gamma^\mu \alpha_\mu$, and the gap function including \hat{x} is characterized as a unit four-vector α_μ (See, Table I). Since the vector type of the gap form represented by α_μ with finite α_i -components ($i = 1, 2, 3$) points to a specific direction, the rotational isotropy is broken except for the rotation around the specific direction, resulting in the anisotropic quasi-particle spectrum below its superconducting transitions, even if the normal state is isotropic. This superconductivity induced anisotropy yields the angle-dependent transport conductivity. For example, the anisotropic thermal conductivity is a clear evidence of the vector type α_μ .²⁷⁾ From the Hamiltonian Eq. (1), the correspondent BdG equations are given as

$$\begin{pmatrix} \gamma^0 \hat{H}^-(\mathbf{r}) & \gamma^0 \Delta^-(\mathbf{r}) \\ \gamma^0 \Delta^+(\mathbf{r}) & \gamma^0 \hat{H}^+(\mathbf{r}) \end{pmatrix} \begin{pmatrix} u(\mathbf{r}) \\ u_c(\mathbf{r}) \end{pmatrix} = E \begin{pmatrix} u(\mathbf{r}) \\ u_c(\mathbf{r}) \end{pmatrix}, \quad (4)$$

where we note that v in the conventional eigen-state form, $(u, v)^T$ is given as $v \equiv i\gamma^2 u_c$.

3. Analytical results

Now, let us examine the vortex-core bound states. In order to analytically concentrate on the low-energy physics, we set the functions as $M(-i\nabla) = M_0$, $P_{1,2,3}(-i\nabla) = -i\bar{P}_{1,2,3}\partial_{x,y,z}$, and $P_0(-i\nabla) = \mu$ (the chemical potential), where M_0 , \bar{P} , and μ are constants. Then, the Dirac Hamiltonian $H^\pm(\mathbf{r})$ is linearized as

$$\hat{H}_{\text{eff}}^\pm(\mathbf{r}) = M_0 - i\partial_x\gamma^1 - i\partial_y\gamma^2 - i\partial_z\gamma^3 \pm \mu\gamma^0, \quad (5)$$

with the rescaled axes $(x, y, z) \rightarrow (\bar{P}_1x, \bar{P}_2y, \bar{P}_3z)$. Hereafter, we do not self-consistently solve the gap equation but just use a well-known analytical form $f(r) = r/\sqrt{r^2 + 1}$ for the radial profile of the gap function given as $\Delta^-(r) \equiv \bar{\Delta}^- f(r)e^{i\theta}$, where θ denotes the polar angle around the vortex line.

At the zero energy, there is a relation expressed as $u_c(\mathbf{r}) = i\gamma^2 u^*(\mathbf{r})$, and the solution of Eq. (4) is given as $u(\mathbf{r}) = \zeta(r)u^N(\mathbf{r})$, where $u^N(r, \theta, z)$ is that of the normal state and $\zeta(r)$ is a scalar real function. In the case of the pseudo-scalar type of gap function $\bar{\Delta}^- = 1$ (so-called $\hat{\Delta}_2$, inter-orbital spin-singlet gap function shown as $\Delta_{\uparrow\downarrow}^{12} = -\Delta_{\downarrow\uparrow}^{12}$, $\Delta_{\uparrow\downarrow}^{21} = -\Delta_{\downarrow\uparrow}^{21}$, $\Delta_{\uparrow\downarrow}^{12} = \Delta_{\uparrow\downarrow}^{21}$ in Ref. 13), there are two bound-state solutions at the zero-energy expressed as

$$u_{\uparrow}(\mathbf{r}) = \frac{e^{-K(r)}}{\sqrt{\lambda_+}} \begin{pmatrix} \sqrt{\mu + M_0}J_0(\bar{r}) \\ 0 \\ 0 \\ ie^{i\theta}\sqrt{\mu - M_0}J_1(\bar{r}) \end{pmatrix}, \quad (6)$$

$$u_{\downarrow}(\mathbf{r}) = \frac{e^{-K(r)}}{\sqrt{\lambda_-}} \begin{pmatrix} 0 \\ e^{i\theta}\sqrt{\mu + M_0}J_1(\bar{r}) \\ -i\sqrt{\mu - M_0}J_0(\bar{r}) \\ 0 \end{pmatrix}, \quad (7)$$

where $\bar{r} \equiv r\sqrt{\mu^2 - M_0^2}$, $K(r) \equiv \int_0^r |f(r')|dr'$, and $J_n(r)$ is the

Table I. Correspondence between our BdG gap functions $\hat{\Delta}^-$ and another representations. ‘‘P-scalar’’ denotes a pseudoscalar whose parity is odd and ‘‘i-polar’’ denotes a polar vector pointing to the i -direction in four-dimensional space.

| | $\hat{\Delta}^-$ | Parity | Fu-Berg ¹⁵⁾ | Sasaki <i>et al.</i> ¹⁴⁾ | energy gap |
|------------|--------------------|--------|------------------------|--|------------|
| Scalar | γ^5 | + | A_{1g} | $\Delta_{1a}: \Delta_{\uparrow\downarrow}^{11} = -\Delta_{\uparrow\downarrow}^{11} = \Delta_{\uparrow\downarrow}^{22} = -\Delta_{\uparrow\downarrow}^{22}$ | full gap |
| t -polar | $\gamma^0\gamma^5$ | + | A_{1g} | $\Delta_{1b}: \Delta_{\uparrow\downarrow}^{11} = -\Delta_{\uparrow\downarrow}^{11} = -\Delta_{\uparrow\downarrow}^{22} = \Delta_{\uparrow\downarrow}^{22}$ | full gap |
| P-scalar | 1 | - | A_{1u} | $\Delta_2: \Delta_{\uparrow\downarrow}^{12} = -\Delta_{\uparrow\downarrow}^{12} = \Delta_{\uparrow\downarrow}^{21} = -\Delta_{\uparrow\downarrow}^{21}$ | full gap |
| x -polar | $\gamma^1\gamma^5$ | - | E_u | $\Delta_{4b}: \Delta_{\uparrow\downarrow}^{12} = -\Delta_{\uparrow\downarrow}^{12} = -\Delta_{\uparrow\downarrow}^{21} = \Delta_{\uparrow\downarrow}^{21}$ | point-node |
| y -polar | $\gamma^2\gamma^5$ | - | E_u | $\Delta_{4a}: \Delta_{\uparrow\downarrow}^{12} = \Delta_{\uparrow\downarrow}^{12} = -\Delta_{\uparrow\downarrow}^{21} = -\Delta_{\uparrow\downarrow}^{21}$ | point node |
| z -polar | $\gamma^3\gamma^5$ | - | A_{2u} | $\Delta_3: \Delta_{\uparrow\downarrow}^{12} = \Delta_{\uparrow\downarrow}^{12} = -\Delta_{\uparrow\downarrow}^{21} = -\Delta_{\uparrow\downarrow}^{21}$ | point node |

Bessel function of the first kind (see the Appendix A). Here, λ_{\pm} is determined by

$$\lambda_{\pm} = 4\pi \int_0^{\infty} dr r e^{-2K(r)} \left[(\mu \pm M_0) J_0(\bar{r})^2 + (\mu \mp M_0) J_1(\bar{r})^2 \right]. \quad (8)$$

Then, one can confirm that the quasi-particle annihilation operators with the zero energy γ_{\uparrow} and γ_{\downarrow} satisfy the Majorana condition $\gamma_{\sigma} = \gamma_{\sigma}^{\dagger}$ because of the relation $u_c(\mathbf{r}) = i\gamma^2 u^*(\mathbf{r})$ (see the Appendix B for more details). It is found that these two solutions are localized when $M_0^2 < \mu^2 + |\Delta_0|^2$.²⁹⁾ Then, we can obtain the solution at finite energy by a perturbation in terms of k_z . The perturbed solution is expressed by the linear combination as $\psi(\mathbf{r})^T = c_{\uparrow}(u_{\uparrow}(\mathbf{r}), u_{c\uparrow}(\mathbf{r}))^T + c_{\downarrow}(u_{\downarrow}(\mathbf{r}), u_{c\downarrow}(\mathbf{r}))^T$. Substituting this solution into Eq. (4), the energy dispersion relations are simply given by

$$E = \pm vk_z, \quad (9)$$

where the coefficients $(c_{\uparrow}, c_{\downarrow}) = (1, \pm i) / \sqrt{2}$ are not dependent on k_z , and

$$v \equiv \frac{4\pi \sqrt{\mu^2 - M_0^2}}{\sqrt{\lambda_+ \lambda_-}} \int_0^{\infty} dr r e^{-2K(r)} (J_0(\bar{r})^2 - J_1(\bar{r})^2). \quad (10)$$

Then, the spin-resolved local densities of states (LDOS's) $n_{\uparrow}(E = vk_z, r) (\equiv |\psi_1(r)|^2 + |\psi_3(r)|^2)$ and $n_{\downarrow}(E = vk_z, r) (\equiv |\psi_2(r)|^2 + |\psi_4(r)|^2)$ are, respectively, expressed as

$$n_{\uparrow}(E = vk_z, r) \equiv \left(\frac{\mu + M_0}{2\lambda_+} + \frac{\mu - M_0}{2\lambda_-} \right) J_0(\bar{r})^2 e^{-2K(r)}, \quad (11)$$

$$n_{\downarrow}(E = vk_z, r) \equiv \left(\frac{\mu - M_0}{2\lambda_+} + \frac{\mu + M_0}{2\lambda_-} \right) J_1(\bar{r})^2 e^{-2K(r)}, \quad (12)$$

where $\psi_i(r)$ is the i -th component of the Dirac spinor $\psi(\mathbf{r})$. The integrated magnetization near a vortex core is also calculated by

$$M_z(r) \sim \int_{-\infty}^0 dE (n_{\uparrow}(E, r) - n_{\downarrow}(E, r)), \quad (13)$$

$$\propto n_{\uparrow}(E \sim 0, r) - n_{\downarrow}(E \sim 0, r). \quad (14)$$

We display r -dependence of n_{\uparrow} and n_{\downarrow} in two parameter sets with the approximated radial function of gap $f(r) = \Delta_0 r / \sqrt{r^2 + 1}$ in Fig. 2.^{30,31)} As seen in Fig. 2(a), n_{\uparrow} in $\mu = 0.4$ eV and $\Delta_0 = 0.3$ eV shows the peak structure at the vortex

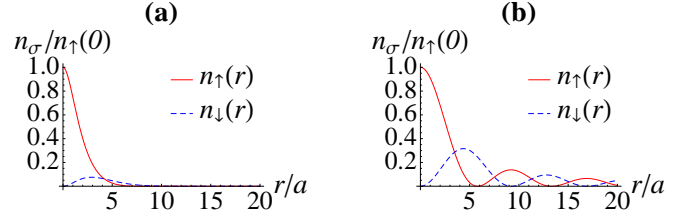


Fig. 2. (Color online) The radial dependence of the spin-resolved zero-energy LDOS's with two calculation parameter sets of (a) $\mu = 0.4$ eV and $\Delta_0 = 0.3$ eV, and (b) $\mu = 0.5$ eV and $\Delta_0 = 0.01$ eV. a is the lattice constant. The spin-resolved LDOS's do not depend on k_z .

center ($r = 0$) in contrast to the zero density in n_{\downarrow} because of $J_0(0) \neq 0$ and $J_1(0) = 0$ in Eqs. (11) and (12). In Fig. 2(b), $\mu = 0.5$ eV and $\Delta_0 = 0.01$ eV, which are the same as those in the previous papers,^{14,27)} n_{\uparrow} and n_{\downarrow} qualitatively behave in similar distribution patterns as shown in Fig. 2(a).

From the results [$n_{\uparrow}(r = 0) > 0$ and $n_{\downarrow}(r = 0) = 0$] and Eq. (14), it is found that $M_z(r = 0) > 0$, *i.e.* the vortex core is spin-polarized. When the gap function is the pseudo-scalar, the spin-polarized vortex *always* emerges because of $n_{\downarrow}(r = 0) = 0$. We note that the local spin imbalance is always satisfied whenever the self-consistent calculation chooses the pseudo-scalar gap function, since $n_{\downarrow}(r = 0) = 0$ is guaranteed by the mathematical constraint on the vortex solution. Though the self-consistent calculation way slightly affects the gap function,^{32,33)} we confirm that the shape of the gap function just changes the intensity of the spin-polarization as discussed later.

4. Numerical results

Next, we numerically calculate the LDOS's with the use of the material parameter sets for $\text{Cu}_x\text{Bi}_2\text{Se}_3$ to compare with the above analytical results. The $L_x \times L_y$ triangle lattice grid is employed, and a single vortex center is located at $(i_x, i_y) = (L_x/2, L_y/2)$. To obtain the LDOS $n(\omega, i_x, i_y)$, we use the spectral polynomial expansion scheme³⁴⁻³⁷⁾ with 40 k_z -points and $L_x = L_y = 96$. We take $a = 30$ eV and $b = -\mu$ as the renormalization factors, $\eta = 1 \times 10^{-3}$ eV as a smearing factor, and $n_c = 8000$ as a cut-off parameter (see, Ref. 36). The gap-amplitude, $\Delta_0 = 0.3$ eV, the chemical potential, $\mu = 0.4$ eV, which are the same as the parameter set of the analyti-

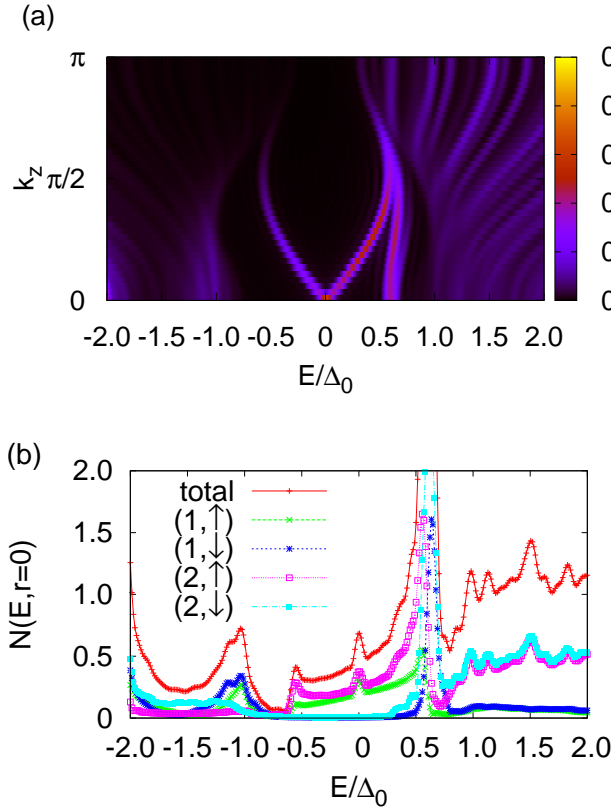


Fig. 3. (Color online) The energy dependence of the LDOS's at the vortex center $(i_x, i_y) = (L_x/2, L_y/2)$ in the pseudo-scalar superconductor. (a) the k_z -resolved LDOS's. (b) the total and partial LDOS's. The total peak reaches the value 4.5 (not shown). The label (l, σ) denotes the σ -spin component with the orbital l .

cal result in Fig. 2(a), and other parameters are the same as those in Ref. 27 (see the Appendix C). In the presence of a vortex, one finds the zero-energy bound states at the vortex center, in which there are k_z -dispersive energy spectra of two bound states as shown in Fig. 3(a). We confirm that a linear dispersion relation develops around the zero-energy while the other has a flat dispersion at the mid-gap energy ($E/\Delta_0 \sim 0.5$). Moreover, it is found that their k_z -dispersive spectra consist of only up-spin quasiparticles while the mid-gap spectrum is opposite (see, Fig. 3(b)). As shown in Fig. 4, r -dependence of the spin-resolved LDOS at the zero-energy around a vortex core reveals that the core is spin-polarized being consistent with our analytical calculation shown in Fig. 2(a).

5. Discussion

5.1 Spin-polarization around a vortex

Finally, we discuss the reason why the Majorana fermion is spin-polarized. It is well known that the state characterized by the zero orbital angular momentum ($L_z = 0$) has the minimum absolute energy with a given k_z around a vortex. On the other hand, the *total* angular momentum \mathbf{J} substitutes for \mathbf{L} in

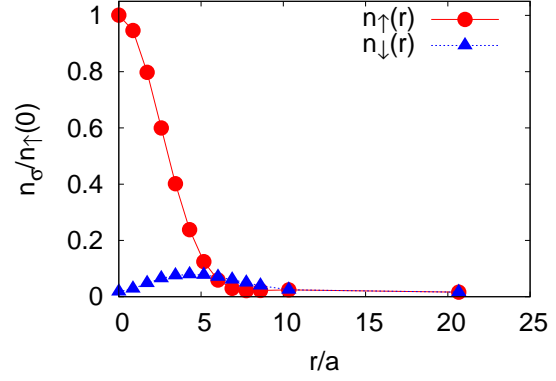


Fig. 4. (Color online) The r -dependence of the spin-resolved LDOS's at the zero-energy in the radial direction from a vortex core. r is rescaled as $r/a = \sqrt{3}(i_x - L_x/2)/(2\bar{A}_2a)$. $i_y = L_y/2$ with $\bar{A}_2a = 4.1$.

the present system according to the spin-orbit coupling. Thus, the bound state with the minimum absolute value of J_z has the minimum absolute energy. The possible total angular momentum is $J_z = 1/2$ or $-1/2$, and which of them is selected as the lowest energy bound state depends on the vortex line direction. It should be noted that the orbital and spin angular momenta \mathbf{L} and \mathbf{S} are not good quantum numbers in this system. Thus, the eigenstate with the minimum $J_z = 1/2$ are given as a linear combination of the two states with $(L_z, S_z) = (0, 1/2)$ and $(1, -1/2)$. This indicates that the $(L_z = 0)$ states including finite k_z -component coincide with $S_z = \frac{1}{2}$. The vortex center is clearly found to be spin-polarized, since the zero angular momentum states have more contribution to the wave function weight at the vortex center ($r = 0$) than non-zero angular momentum states (i.e., $J_0(r = 0) > J_1(r = 0)$). Thus, we conclude that the zero-energy Majorana fermion is distinctly spin-polarized in the vortex core and the core itself is also spin-polarized ($M_z(r = 0) > 0$). The spin-polarized core is easily observable if a vortex lattice is formed. For example, the neutron or muon scattering is sensitive to such spin-density lattice modulations, and NMR is also a good probe.

A spin-polarized core never occur in the even parity scalar-type superconductivity (so-called Δ_1 shown as $\Delta_{\uparrow\downarrow}^{11} = -\Delta_{\uparrow\downarrow}^{11}$, $\Delta_{\uparrow\downarrow}^{22} = -\Delta_{\uparrow\downarrow}^{22}$, $\Delta_{\uparrow\downarrow}^{11} = \Delta_{\uparrow\downarrow}^{22}$ in Ref. 13), since a bound state has finite energy and consists of the Bessel function with half integers (e.g. $J_{n\pm 1/2}(r)$). In other odd-parity superconductors with polar-vector-type gap functions, spin-polarized Majorana bound states occur in magnetic fields parallel to a direction of the point-nodes.

Here, we discuss whether a spin-polarization can occur even for nonzero energy bound states in a vortex core which are not Majorana bound states. There are two kinds of finite energy bound states. One is a bound state with a zero angular momentum and finite k_z , whose spin-resolved LDOS is expressed in Eqs. (11) and (12). This bound state is spin-polarized and a integrated magnetization Eq. (14) is finite. The other is a bound state with a finite angular momentum,

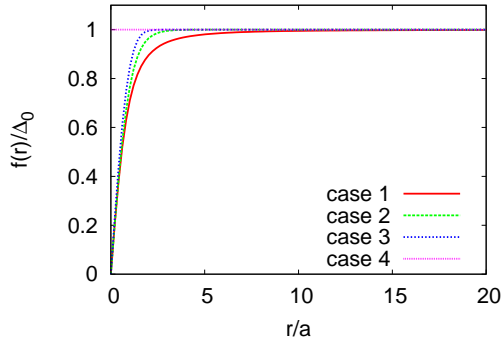


Fig. 5. (Color online) Various kinds of the functions $f(r)$ determined in Eq. (15).

which can not be obtained analytically. This state consists of the Bessel functions with finite integers, i.e. $J_n(r)$ and $J_{n+1}(r)$. A spin imbalance of a finite angular momentum state might be smaller than that of a zero angular momentum state at a vortex center because of $J_n(r=0) = J_{n+1}(r=0) = 0$.

5.2 Robustness of the spin-polarized Majorana bound states

We show the robustness of the spin-polarized Majorana bound states. In general, solving the gap equations closes the self-consistent calculations in the Bogoliubov-de Gennes formalism. We adopt the approximated radial function of gap $f(r) = \Delta_0 r / \sqrt{r^2 + 1}$ in the previous section. The self-consistent calculation yields the correct form of $f(r)$. We have to show that the self-consistent calculation does not change our results. However, one can not determine the parameters in the gap equations, since the kind of the pairing interaction for $\text{Cu}_x\text{Bi}_2\text{Se}_3$ has not been determined in experiments. Therefore, we show the $f(r)$ -dependence of the spin-polarized bound states in this section. The correct form of the function $f(r)$ must satisfy the condition of $f(r=0) = 0$ and $\lim_{r \rightarrow \infty} f(r) = \Delta_0$. We consider the several functions as follows (See, Fig. 5):

$$f(r) = \begin{cases} \Delta_0 \frac{r}{\sqrt{r^2 + 1}} & \text{(case 1)} \\ \Delta_0 \tanh(r) & \text{(case 2)} \\ \Delta_0 \text{Erf}(r) & \text{(case 3)} \\ \Delta_0 & \text{(case 4)} \end{cases} . \quad (15)$$

As shown in Fig. 6, we can conclude that the results do not depend on the form of $f(r)$ in terms of the spin-polarization.

6. Conclusion

In conclusion, we examined vortex core bound-states in the topological superconductors. With the use of the analytical and numerical calculations, we found that the zero-energy Majorana fermions are spin-polarized and the vortex core itself is distinctly magnetized when the rotational symmetry around the vortex line is preserved. The result is universal for Dirac superconductivity whose rotational degree of freedom

is characterized by total angular momentum $J = S + L$. Such a drastic feature is easily observable in experiments.

Acknowledgment

We thank M. Okumura for helpful discussions and comments. The calculations were performed using the supercomputing system PRIMERGY BX900 at the Japan Atomic Energy Agency. This study was supported by Grants-in-Aid for Scientific Research from MEXT of Japan.

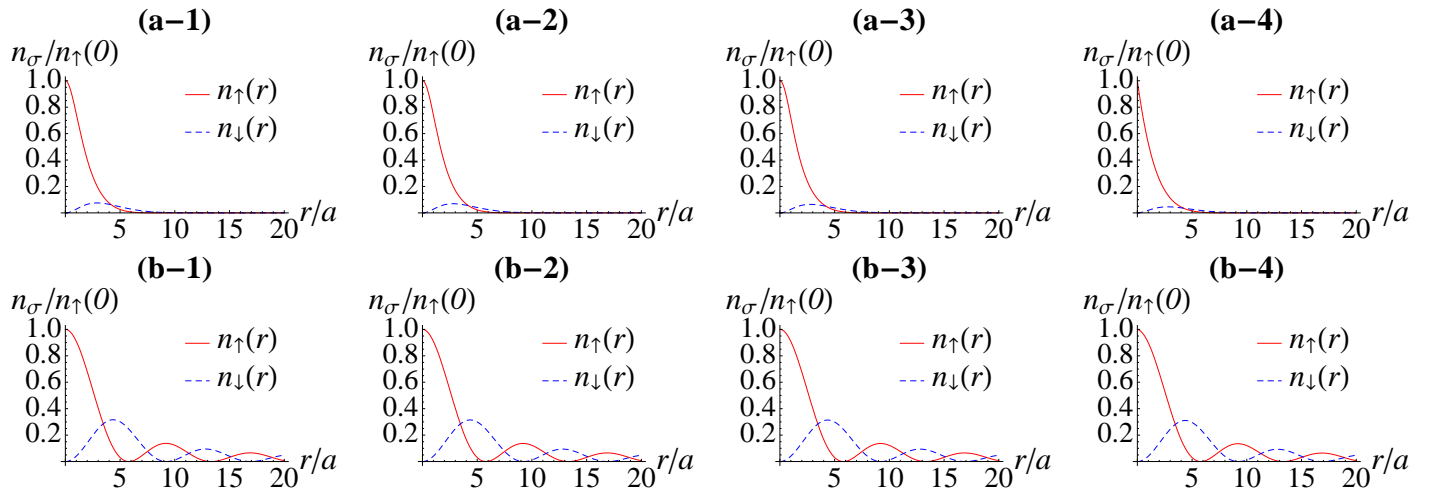


Fig. 6. (Color online) The radial dependence of the spin-resolved zero-energy LDOS's with two calculation parameter sets of (a) $\mu = 0.4\text{eV}$ and $\Delta_0 = 0.3\text{eV}$, and (b) $\mu = 0.5\text{eV}$ and $\Delta_0 = 0.01\text{eV}$. a is the lattice constant. The function $f(r)$ in Eq. (15) is adopted, respectively.

Appendix A: Solutions of the BdG equation around a vortex

Let us solve the following BdG equations:

$$\hat{H} \begin{pmatrix} u(\mathbf{r}) \\ u_c(\mathbf{r}) \end{pmatrix} = E \begin{pmatrix} u(\mathbf{r}) \\ u_c(\mathbf{r}) \end{pmatrix}, \quad (\text{A}\cdot 1)$$

where the Hamiltonian is

$$\hat{H} = \begin{pmatrix} \gamma^0 \hat{H}^-(\mathbf{r}) & \gamma^0 \Delta^-(\mathbf{r}) \\ \gamma^0 \Delta^+(\mathbf{r}) & \gamma^0 \hat{H}^+(\mathbf{r}) \end{pmatrix} = \begin{pmatrix} \hat{h}(\mathbf{r}) - \mu & \Delta'(\mathbf{r}) \\ \Delta'^{\dagger} & \hat{h}(\mathbf{r}) + \mu \end{pmatrix}, \quad (\text{A}\cdot 2)$$

with

$$\hat{h}(\mathbf{r}) = \gamma^0 M_0 - i\partial_x \gamma^0 \gamma^1 - i\partial_y \gamma^0 \gamma^2 - i\partial_z \gamma^0 \gamma^3. \quad (\text{A}\cdot 3)$$

It should be noted that one can find the solution $(u^-, u_c^-) = (i\gamma^2 u_c^*, i\gamma^2 u^*)$ with the energy $-E$ when (u, u_c) is a solution with the energy E . The zero-energy solutions satisfy the following equations,

$$(\hat{h} - \mu)u + \Delta' i\gamma^2 u^* = 0, \quad (\text{A}\cdot 4)$$

$$\Delta'^{\dagger} i\gamma^2 u_c^* + (\hat{h} + \mu)u_c = 0. \quad (\text{A}\cdot 5)$$

We assume that these solutions are expressed as

$$u(\mathbf{r}) = \zeta(r) u^N(r, \theta, z). \quad (\text{A}\cdot 6)$$

Here, $u^N(r, \theta, z)$ is a solution in the normal states which satisfies

$$(\hat{h} - \mu)u^N(\mathbf{r}) = 0. \quad (\text{A}\cdot 7)$$

At first, we solve the equation in the normal states. The equation is rewritten as

$$\hat{h}^2 u^N(\mathbf{r}) = \mu^2 u^N(\mathbf{r}), \quad (\text{A}\cdot 8)$$

$$(-\nabla^2 + M_0^2)u^N(\mathbf{r}) = \mu^2 u^N(\mathbf{r}). \quad (\text{A}\cdot 9)$$

Thus, each component of the solution is expressed as

$$u^{\text{Ni}}(\mathbf{r}) = c_i e^{in_i \theta} J_{n_i}(\alpha r) e^{ik_z z}, \quad (\text{A}\cdot 10)$$

with $\alpha \equiv \sqrt{\mu^2 - M_0^2 - k_z^2}$. In order to obtain coefficients (c_1, c_2, c_3, c_4) , we solve the following equations,

$$\begin{pmatrix} M_0 & 0 & k_z & L_- \\ 0 & M_0 & L_+ & -k_z \\ k_z & L_- & -M_0 & 0 \\ L_+ & -k_z & 0 & -M_0 \end{pmatrix} \begin{pmatrix} c_1 e^{in_1\theta} J_{n_1}(\alpha r) \\ c_2 e^{in_2\theta} J_{n_2}(\alpha r) \\ c_3 e^{in_3\theta} J_{n_3}(\alpha r) \\ c_4 e^{in_4\theta} J_{n_4}(\alpha r) \end{pmatrix} e^{ik_z z} = \mu \begin{pmatrix} c_1 e^{in_1\theta} J_{n_1}(\alpha r) \\ c_2 e^{in_2\theta} J_{n_2}(\alpha r) \\ c_3 e^{in_3\theta} J_{n_3}(\alpha r) \\ c_4 e^{in_4\theta} J_{n_4}(\alpha r) \end{pmatrix} e^{ik_z z}, \quad (\text{A}\cdot 11)$$

with

$$L_{\pm} \equiv \pm e^{\pm i\theta} \left(\mp i \frac{\partial}{\partial r} + \frac{1}{r} \frac{\partial}{\partial \theta} \right). \quad (\text{A}\cdot 12)$$

With the use of the relations $\partial_r J_n(r) = -J_{n+1}(r) + (n/r)J_n(r)$ and $\partial_r J_n(r) = J_{n-1}(r) - (n/r)J_n(r)$, we obtain

$$L_{\pm} e^{in\theta} J_n(\alpha r) = \pm e^{i(n\pm 1)\theta} \left(\mp i \frac{\partial}{\partial r} + \frac{in}{r} \right) J_n(\alpha r) \quad (\text{A}\cdot 13)$$

$$= \pm e^{i(n\pm 1)\theta} i\alpha J_{n\pm 1}(\alpha r). \quad (\text{A}\cdot 14)$$

Thus, the equations are rewritten as

$$\begin{pmatrix} (M_0 - \mu) e^{in_1\theta} J_{n_1}(\alpha r) & 0 & k_z e^{in_3\theta} J_{n_3}(\alpha r) & -e^{i(n_4-1)\theta} i\alpha J_{n_4-1}(\alpha r) \\ 0 & (M_0 - \mu) e^{in_2\theta} J_{n_2}(\alpha r) & e^{i(n_3+1)\theta} i\alpha J_{n_3+1}(\alpha r) & -k_z e^{in_4\theta} J_{n_4}(\alpha r) \\ k_z e^{in_1\theta} J_{n_1}(\alpha r) & -e^{i(n_2-1)\theta} i\alpha J_{n_2-1}(\alpha r) & (-M_0 - \mu) e^{in_3\theta} J_{n_3}(\alpha r) & 0 \\ e^{i(n_1+1)\theta} i\alpha J_{n_1+1}(\alpha r) & -k_z e^{in_2\theta} J_{n_2}(\alpha r) & 0 & (-M_0 - \mu) e^{in_4\theta} J_{n_4}(\alpha r) \end{pmatrix} \begin{pmatrix} c_1 \\ c_2 \\ c_3 \\ c_4 \end{pmatrix} = 0. \quad (\text{A}\cdot 15)$$

The orbital angular momenta n_i must satisfy

$$n_2 = n_1 + 1, \quad n_3 = n_1, \quad n_4 = n_1 + 1. \quad (\text{A}\cdot 16)$$

Then, in the case of $k_z = 0$, the coefficients are written as

$$c_3 = -\frac{ic_2\alpha}{M_0 + \mu}, \quad c_4 = \frac{ic_1\alpha}{M_0 + \mu}. \quad (\text{A}\cdot 17)$$

We assume that $\zeta(r)$ in Eq. (A-6) is a real scalar function. By substituting Eq. (A-6) into the differential equations Eq. (A-4), we obtain

$$\begin{pmatrix} ie^{-i\theta} \frac{\partial \zeta(r)}{\partial r} \frac{ic_1\alpha}{M_0 + \mu} e^{i(n_1+1)\theta} J_{n_1+1}(\alpha r) \\ -ie^{i\theta} \frac{\partial \zeta(r)}{\partial r} \frac{ic_2\alpha}{M_0 + \mu} e^{in_1\theta} J_{n_1}(\alpha r) \\ ie^{-i\theta} \frac{\partial \zeta(r)}{\partial r} c_2 e^{i(n_1+1)\theta} J_{n_1+1}(\alpha r) \\ ie^{i\theta} \frac{\partial \zeta(r)}{\partial r} c_1 e^{in_1\theta} J_{n_1}(\alpha r) \end{pmatrix} + \zeta(r) \Delta'(r) \begin{pmatrix} \frac{-ic_1^*\alpha}{M_0 + \mu} e^{-i(n_1+1)\theta} J_{n_1+1}(\alpha r) \\ \frac{ic_2^*\alpha}{M_0 + \mu} e^{-in_1\theta} J_{n_1}(\alpha r) \\ -c_2^* e^{-i(n_1+1)\theta} J_{n_1+1}(\alpha r) \\ -c_1^* e^{-in_1\theta} J_{n_1}(\alpha r) \end{pmatrix} = 0 \quad (\text{A}\cdot 18)$$

Finally, we consider the gap function represented by a pseudo-scalar. In this case, $\Delta'(r)$ with a vortex is expressed as

$$\Delta'(r) = f(r) e^{iM\theta} \gamma^0. \quad (\text{A}\cdot 19)$$

Here, M is a winding number and $f(r)$ is the amplitude of the order parameters ($f(r=0) = 0$ and $f(r) > 0$). By substituting $\Delta'(r)$ into the above differential equations, we obtain

$$\begin{pmatrix} i \frac{\partial \zeta(r)}{\partial r} \frac{ic_1\alpha}{M_0 + \mu} e^{in_1\theta} J_{n_1+1}(\alpha r) \\ -i \frac{\partial \zeta(r)}{\partial r} \frac{ic_2\alpha}{M_0 + \mu} e^{i(n_1+1)\theta} J_{n_1}(\alpha r) \\ i \frac{\partial \zeta(r)}{\partial r} c_2 e^{in_1\theta} J_{n_1+1}(\alpha r) \\ i \frac{\partial \zeta(r)}{\partial r} c_1 e^{i(n_1+1)\theta} J_{n_1}(\alpha r) \end{pmatrix} + \zeta(r) f(r) \begin{pmatrix} \frac{-ic_1^*\alpha}{M_0 + \mu} e^{i(-n_1-1+M)\theta} J_{n_1+1}(\alpha r) \\ \frac{ic_2^*\alpha}{M_0 + \mu} e^{i(-n_1+M)\theta} J_{n_1}(\alpha r) \\ -c_2^* e^{i(-n_1-1+M)\theta} J_{n_1+1}(\alpha r) \\ -c_1^* e^{i(-n_1+M)\theta} J_{n_1}(\alpha r) \end{pmatrix} = 0. \quad (\text{A}\cdot 20)$$

The angular momentum of the zero energy solutions is

$$n_1 = \frac{M-1}{2}. \quad (\text{A}\cdot 21)$$

Since $\zeta(r)$ is a scalar real function, we obtain two solutions with coefficients

$$(c_1, c_2) = (|c_1| \exp\left[\frac{\pi i}{4}\right], 0), \quad (0, |c_2| \exp\left[-\frac{\pi i}{4}\right]). \quad (\text{A}\cdot 22)$$

Therefore, the zero-energy solutions with a winding number M are written as

$$u_{\uparrow}(\mathbf{r}) = c_{\uparrow} e^{-K(r)} \begin{pmatrix} b_{+} \exp\left[i\frac{M-1}{2}\theta\right] J_{\frac{M-1}{2}}(ar) \\ 0 \\ 0 \\ ib_{-} \exp\left[i\frac{M+1}{2}\theta\right] J_{\frac{M+1}{2}}(ar) \end{pmatrix}, \quad (\text{A}\cdot 23)$$

$$u_{\downarrow}(\mathbf{r}) = c_{\downarrow} e^{-K(r)} \begin{pmatrix} 0 \\ b_{+} \exp\left[i\frac{M+1}{2}\theta\right] J_{\frac{M+1}{2}}(ar) \\ -ib_{-} \exp\left[i\frac{M-1}{2}\theta\right] J_{\frac{M-1}{2}}(ar) \\ 0 \end{pmatrix}, \quad (\text{A}\cdot 24)$$

with $a = \sqrt{\mu^2 - M_0^2}$, $b_{\pm} = \sqrt{\mu \pm M_0}$ and $K(r) = \int_0^r |f(r')| dr'$.

Appendix B: Proof of the Majorana condition

In terms of the BdG equations, the quasiparticle annihilation operator γ_{σ} with the zero energy is expressed as

$$\gamma_{\sigma} = \int d\mathbf{r} \left\{ u_{\sigma}^{\text{T}}(\mathbf{r}) \psi(\mathbf{r}) + u_{\text{c},\sigma}^{\text{T}} \psi_{\text{c}}(\mathbf{r}) \right\}. \quad (\text{B}\cdot 1)$$

Here, $\psi_{\text{c}} = i\gamma^2(\psi^{\dagger})^{\text{T}}$. At the zero energy, there is a relation expressed as $u_{\text{c},\sigma}(\mathbf{r}) = i\gamma^2 u_{\sigma}^*(\mathbf{r})$. Substituting the above relation into eq. (B·1), the quasiparticle creation operator $\gamma_{\sigma}^{\dagger}$ is written as

$$\gamma_{\sigma}^{\dagger} = \int d\mathbf{r} \left\{ \psi(\mathbf{r})^{\dagger} u_{\sigma}^*(\mathbf{r}) + \left[\psi^{\text{T}}(\mathbf{r}) (i\gamma^2)^{\dagger} \right] \left[i\gamma^2 \right]^* u_{\sigma}^*(\mathbf{r}) \right\}, \quad (\text{B}\cdot 2)$$

$$= \gamma_{\sigma}. \quad (\text{B}\cdot 3)$$

Thus, the quasiparticle creation operator $\gamma_{\sigma}^{\dagger}$ with the zero energy eigenvalue satisfies the Majorana condition.

Appendix C: Parameters in numerical calculations

We show the parameters in numerical calculations. The mean-field Hamiltonian on the triangular lattice based on the Bogoliubov-de Gennes formalism is expressed as

$$H = \sum_{k_z} \sum_{i,j} \begin{pmatrix} c_i^\dagger & c_i^T \end{pmatrix} \begin{pmatrix} \hat{H}_{ij}(k_z) & \hat{\Delta}f(\mathbf{R}_i)\delta_{ij} \\ \hat{\Delta}^\dagger\delta_{ij}f(\mathbf{R}_i)^* & -\hat{H}_{ij}^*(-k_z) \end{pmatrix} \begin{pmatrix} c_j \\ c_j^* \end{pmatrix}, \quad (\text{C}\cdot 1)$$

where c_i^\dagger is the 4-component creation operator at the i -th site on the two-dimensional triangle lattice and k_z denotes the momentum in the crystal c -axis. $\hat{\Delta} = \gamma^0\Delta^-i\gamma^2\gamma^0$ is 4×4 matrix whose elements are given as $\Delta_{\sigma\sigma'}^{lm}$ with orbital $l(m)$ and spin $\sigma(\sigma')$ indices. The normal state Hamiltonian $\hat{H}_{ij}(k_z)$ is given by

$$\hat{H}_{ij}(k_z) = \int d\mathbf{k}_\perp e^{i\mathbf{k}_\perp \cdot (\mathbf{R}_i - \mathbf{R}_j)} \hat{H}(\mathbf{k}_\perp, k_z), \quad (\text{C}\cdot 2)$$

with ab -plane momentum $\mathbf{k}_\perp = (k_x, k_y)$. The 4×4 matrix $\hat{H}(\mathbf{k}_\perp, k_z)$ is expressed as

$$\begin{aligned} \hat{H}(\mathbf{k}_\perp, k_z) &= M(\mathbf{k}_\perp, k_z)\gamma^0 + P_0(\mathbf{k}_\perp, k_z) \\ &+ \gamma^0 P_1(\mathbf{k}_\perp)\gamma^1 + \gamma^0 P_2(\mathbf{k}_\perp)\gamma^2 + \gamma^0 P_3(k_z)\gamma^3, \end{aligned} \quad (\text{C}\cdot 3)$$

where,

$$M(\mathbf{k}_\perp, k_z) \equiv M_0 - 2\bar{B}_1(1 - \cos(k_z)) - \bar{B}_2\eta(\mathbf{k}_\perp), \quad (\text{C}\cdot 4)$$

$$P_0(\mathbf{k}_\perp, k_z) \equiv 2\bar{D}_1(1 - \cos(k_z)) + \bar{D}_2\eta(\mathbf{k}_\perp) - \mu, \quad (\text{C}\cdot 5)$$

$$P_1(\mathbf{k}_\perp) \equiv \frac{2}{3}\bar{A}_2\sqrt{3}\sin\left(\frac{\sqrt{3}}{2}k_x\right)\cos\left(\frac{k_y}{2}\right), \quad (\text{C}\cdot 6)$$

$$P_2(\mathbf{k}_\perp) \equiv \frac{2}{3}\bar{A}_2\left(\cos\left(\frac{\sqrt{3}}{2}k_x\right)\sin\left(\frac{k_y}{2}\right) + \sin(k_y)\right), \quad (\text{C}\cdot 7)$$

$$P_3(k_z) \equiv \bar{A}_1\sin(k_z), \quad (\text{C}\cdot 8)$$

with $\eta(\mathbf{k}_\perp) \equiv (3 - 2\cos(\sqrt{3}k_x/2)\cos(k_y/2) - \cos(k_y))$. We set $M_0 = 0.28$ eV, $\bar{A}_1 = 0.32$ eV, $\bar{A}_2 = 4.1/a$ eV, $\bar{B}_1 = 0.216$ eV, $\bar{B}_2 = 56.6/a^2$ eV, $\bar{D}_1 = 0.024$ eV, $\bar{D}_2 = 19.6/a^2$ and $a = 4.076$ Å as the material parameters for $\text{Cu}_x\text{Bi}_2\text{Si}_3$. For simplicity, we do not solve the gap-equation but use a spatial distribution form of the order parameter around a single vortex $f(\mathbf{R}_i)$ written as

$$f(\mathbf{R}_i) = e^{i\theta}\Delta_0\frac{|\mathbf{R}_i|}{\sqrt{|\mathbf{R}_i|^2 + \xi^2}}, \quad (\text{C}\cdot 9)$$

where θ denotes the polar angle around c -axis, Δ_0 is the amplitude of the order-parameter and ξ is the coherence length.

- 2) B. A. Bernevig, T. L. Hughes, and S.-C. Zhang, *Science* **314**, 1757 (2006).
- 3) Y. L. Chen, Z. K. Liu, J. G. Analytis, J.-H. Chu, H. J. Zhang, B. H. Yan, S.-K. Mo, R. G. Moore, D. H. Lu, I. R. Fisher, S. C. Zhang, Z. Hussain, and Z.-X. Shen, *Phys. Rev. Lett.* **105**, 266401 (2010).
- 4) L. Fu and C. L. Kane, *Phys. Rev. B* **76**, 045302 (2007).
- 5) L. Fu, C. L. Kane, and E. J. Mele, *Phys. Rev. Lett.* **98**, 106803 (2007).
- 6) M. Z. Hasan and C. L. Kane, *Rev. Mod. Phys.* **82**, 3045 (2010), and references therein.
- 7) C. L. Kane and E. J. Mele, *Phys. Rev. Lett.* **95**, 146802 (2005).
- 8) M. König, S. Wiedmann, C. Brüne, A. Roth, H. Buhmann, L. W. Molenkamp, X.-L. Qi, and S.-C. Zhang, *Science* **318**, 766 (2007).
- 9) K. Kuroda, M. Ye, A. Kimura, S. V. Ereemeev, E. E. Krasovskii, E. V. Chulkov, Y. Ueda, K. Miyamoto, T. Okuda, K. Shimada, H. Namatame, and M. Taniguchi, *Phys. Rev. Lett.* **105**, 146801 (2010).
- 10) J. E. Moore and L. Balents, *Phys. Rev. B* **75**, 121306 (2007).
- 11) A. Nishide, A. A. Taskin, Y. Takeichi, T. Okuda, A. Kakizaki, T. Hirahara, K. Nakatsuji, F. Komori, Y. Ando, and I. Matsuda, *Phys. Rev. B* **81**, 041309 (2010).
- 12) T. Sato, K. Segawa, H. Guo, K. Sugawara, S. Souma, T. Takahashi, and Y. Ando, *Phys. Rev. Lett.* **105**, 136802 (2010).
- 13) S. Sasaki, Z. Ren, A. A. Taskin, K. Segawa, L. Fu, and Y. Ando, *Phys. Rev. Lett.* **109**, 217004 (2012).
- 14) S. Sasaki, M. Kriener, K. Segawa, K. Yada, Y. Tanaka, M. Sato, and Y. Ando, *Phys. Rev. Lett.* **107**, 217001 (2011).
- 15) L. Fu and E. Berg, *Phys. Rev. Lett.* **105**, 097001 (2010).
- 16) Y. S. Hor, A. J. Williams, J. G. Checkelsky, P. Roushan, J. Seo, Q. Xu, H. W. Zandbergen, A. Yazdani, N. P. Ong, and R. J. Cava, *Phys. Rev. Lett.* **104**, 057001 (2010).
- 17) T. Kirzhner, E. Lahoud, K. B. Chaska, Z. Salman, and A. Kanigel, *Phys. Rev. B* **86**, 064517 (2012).
- 18) L. A. Wray, S.-Y. Xu, Y. Xia, Y. S. Hor, D. Qian, A. V. Fedorov, H. Lin, A. Bansil, R. J. Cava, and M. Z. Hasan, *Nat Phys* **6**, 855 (2010).
- 19) T. H. Hsieh, H. Lin, J. Liu, W. Duan, A. Bansil, and L. Fu, *Nat Commun* **3**, 982 (2012).
- 20) M. Kriener, K. Segawa, Z. Ren, S. Sasaki, and Y. Ando, *Phys. Rev. Lett.* **106**, 127004 (2011).
- 21) M. Sigrist, A. Furusaki, C. Honerkamp, M. Matsumoto, K.-K. Ng, and Y. Okuno, *J. Phys. Soc. Jpn. Supple. B* **89**, 127 (2000).
- 22) Y. Nagai and N. Hayashi, *Phys. Rev. B* **79**, 224508 (2009).
- 23) Y. Tanaka and S. Kashiwaya, *Phys. Rev. Lett.* **74**, 3451 (1995).
- 24) M. Matsumoto and R. Heeb, *Phys. Rev. B* **65**, 014504 (2001).
- 25) M. Takigawa, M. Ichioka, K. Machida, and M. Sigrist, *Phys. Rev. B* **65**, 014508 (2001).
- 26) L. Hao and T. K. Lee, *Phys. Rev. B* **83**, 134516 (2011).
- 27) Y. Nagai, H. Nakamura, and M. Machida, *Phys. Rev. B* **86**, 094507 (2012).
- 28) D. Sticlet, C. Bena, and P. Simon, *Phys. Rev. Lett.* **108**, 096802 (2012).
- 29) Y. Nishida, *Phys. Rev. D* **81**, 074004 (2010).
- 30) A. S. Mel'nikov, D. A. Ryzhov, and M. A. Silaev, *Phys. Rev. B* **78**, 064513 (2008).
- 31) Y. Nagai, H. Nakamura, and M. Machida, *Phys. Rev. B* **83**, 104523 (2011).
- 32) F. Gygi and M. Schlüter, *Phys. Rev. B* **43**, 7609 (1991).
- 33) F. Gygi and M. Schlüter, *Phys. Rev. Lett.* **65**, 1820 (1990).
- 34) L. Covaci, F. M. Peeters, and M. Berciu, *Phys. Rev. Lett.* **105**, 167006 (2010).
- 35) Y. Nagai, N. Nakai, and M. Machida, *Phys. Rev. B* **85**, 092505 (2012).
- 36) Y. Nagai, Y. Ota, and M. Machida, *J. Phys. Soc. Jpn.* **81**, 024710 (2012).
- 37) A. Weiße, G. Wellein, A. Alvermann, and H. Fehske, *Rev. Mod. Phys.* **78**, 275 (2006).

1) J. C. Y. Teo and C. L. Kane, *Phys. Rev. Lett.* **104**, 046401 (2011).